

Covariant Boltzmann-Uehling-Uhlenbeck approach for heavy-ion collisions

Bernhard Blättel, Volker Koch, Wolfgang Cassing, and Ulrich Mosel

Institut für Theoretische Physik, Justus-Liebig-Universität Giessen, 6300 Giessen, Federal Republic of Germany

(Received 28 April 1988)

We present a covariant transport theory for heavy-ion collisions based on the σ - ω model. The two-body collision term is introduced in line with relativistic classical kinetic theory assuming the free nucleon-nucleon cross section in the collision integral. Within this approach, we study collisions of $^{16}\text{O} + ^{16}\text{O}$ at 600 MeV/nucleon for two different parameter sets of the underlying Lagrangian density, i.e., different equations of state. The most striking result is the strong sensitivity of the transverse momentum distribution on the momentum dependence of the mean field which is self-consistently included in the relativistic approach. We find that residual two-particle collisions might even slightly reduce the transverse momentum p_t due to an increase of stopping power obtained from the collisions. An increase of the cross section by a factor of 2 leads to a much smaller enhancement of p_t than observed in nonrelativistic calculations with a momentum independent mean field. We furthermore present a first application to high-energy photon production and study the influence of the equation of state on the differential photon yield.

I. INTRODUCTION

It is one of today's major goals in nuclear physics to extract information about the strong interactions, especially the nuclear equation of state (EOS) via the investigation of heavy-ion collisions. A lot of effort in this direction has been done by applying transport theoretical techniques like simulations of the Boltzmann-Uehling-Uhlenbeck (BUU) equation. These simulations combine the complementary mean field and cascade description for heavy-ion collisions at the semiclassical level. However, to obtain reliable information about the EOS at high densities the theoretical description has to be improved in several aspects.

It is known from nucleon-nucleus scattering,¹ as well as from the Brueckner theory,² that the nuclear potential felt by a nucleon depends on its momentum. It becomes less attractive if the nucleon momentum increases. It has been shown that this momentum dependence of the mean-field potential can significantly alter the results of BUU calculations concerning properties like momentum flow and particle production.³ It is therefore desirable to start from a theory that takes the static mean field and its momentum dependence consistently into account. Furthermore, a change of the nucleon-nucleon collision cross section due to medium effects⁴ may influence the results.⁵ Finally, to probe the high-density region of nuclear matter, relativistic bombarding energies are necessary which certainly require a covariant description. Besides the relativistic kinematics this especially involves a relativistic formulation of the mean-field forces thus avoiding shortcomings like, e.g., superluminal velocities of sound as they are observed by the nonrelativistic Skryme forces at higher densities.⁶

In the following we therefore investigate a model which is formulated fully covariantly and thus naturally includes momentum dependent forces.^{7,8} On the basis of the σ - ω model (QHD I) (Ref. 9) a covariant Vlasov equa-

tion can be formulated.¹⁰ In Sec. II we briefly review this derivation and propose a two-body collision term motivated by the covariant classical kinetic theory.¹¹ In this way we obtain the simplest version of a relativistic transport theory for heavy-ion collisions.¹² A similar approach has been recently proposed by Ko *et al.*¹³

The numerical realization is discussed in Sec. III. The results from the pure Vlasov part and the effects from the two-particle collisions will be shown in Sec. IV. Besides the time evolution of the densities we will concentrate on momentum space, especially the transverse momentum distributions and the rapidity spectrum. Finally we apply the model to the production of high-energy photons as a first application to two-body observables.

II. A COVARIANT BUU APPROACH

A. The covariant streaming term

We start out with a field theoretical model of nucleons coupled to scalar and vector mesons (QHD I) given by the following Lagrangian density as proposed in⁹

$$\begin{aligned} \mathcal{L}_W = & \bar{\Psi}[\gamma_\mu(i\partial^\mu - g_v\omega^\mu) - (M_s - g_s\Phi)]\Psi \\ & + \frac{1}{2}\partial_\mu\Phi\partial^\mu\Phi - \frac{1}{2}m_s^2\Phi^2 - \frac{B}{3}\Phi^3 - \frac{C}{4}\Phi^4 \\ & - \frac{1}{4}F_{\mu\nu}F^{\mu\nu} + \frac{1}{2}m_v^2\omega_\mu\omega^\mu, \end{aligned} \quad (1)$$

where we have further included a nonlinear self-interaction of the scalar field.¹⁴ In this simplest version of the model it is sufficient to treat only the four Dirac components of the nucleon spinor explicitly, since the interaction is invariant under rotations in isospin space.

In the following we treat this Lagrangian in the Hartree approximation. This means that the meson fields are treated as classical fields and one obtains equations of motion for the c -number-valued meson fields and nucleon

spinors. In the present approach we further neglect nucleonic negative energy states. With these approximations the model is known to describe the saturation of nuclear matter and static properties of nuclei reasonably well.⁹ It also contains a momentum dependence of the interaction whose strength is determined by the same parameters as the static mean field. The investigation of nucleon-nucleus scattering in this model shows that the optical potential increases linearly with the energy of the nucleon.⁹ The steepness of this rise depends on the inverse of the Fermi-liquid effective mass which is close to the relativistic effective mass $m^* = M - g_s \Phi$ in nuclear matter.^{15,8} Thus, a low effective mass leads to a strong momentum dependence.

It is our aim to describe the time evolution of finite systems of nucleons via a one-particle distribution function which, in the classical limit, goes over to a phase-space distribution function. We therefore introduce the Wigner matrix

$$W_{\alpha\beta} = \frac{1}{(2\pi)^4} \int d^4R e^{-ip_\mu R^\mu} \bar{\Psi}_\beta \left[x + \frac{R}{2} \right] \Psi_\alpha \left[x - \frac{R}{2} \right], \quad (2)$$

where Ψ_α denotes the spinor component, i.e., $\alpha=0,1,2,3$. Starting from the Dirac equation, an equation of motion for $W(x,p)$ can be derived.¹⁰ To simplify the coupled equations for $W_{\alpha\beta}$ we introduce the following spinor decomposition

$$W = \mathcal{F} + \gamma_\mu \mathcal{V}^\mu + \frac{1}{2} \sigma_{\mu\nu} \mathcal{S}^{\mu\nu}, \quad (3)$$

where we use that the pseudoscalar and the axial vector part vanish for spin saturated system.¹⁶ The resulting equations are then considered in the classical limit $\hbar \rightarrow 0$. More precisely, this involves the following two approximations. One of them is an expansion up to first order in the "triangle operator" $\hbar \Delta = \hbar \partial_\mu^x \partial_p^\mu$, where the spatial derivative of the triangle operator acts only on the meson fields. It is valid if

$$\hbar \ll \Delta R_{\Phi,\omega} \Delta P_W, \quad (4)$$

where $\Delta R_{\Phi,\omega}, \Delta P_W$ are intervals in which the fields and the Wigner matrix significantly change in coordinate and momentum space, respectively. In a second step one further assumes that the Wigner matrix is also slowly varying in coordinate space within the Compton wavelength of the nucleon.

We obtain the relativistic Vlasov equation

$$\{ \Pi_\mu \partial^\mu + [g_v \Pi_\nu F^{\mu\nu} + m^* (\partial_x^\mu m^*)] \partial_\mu^\Pi \} f(x, \Pi) = 0 \quad (5)$$

together with the mass shell constraint

$$(\Pi^2 - m^{*2}) f(x, \Pi) = 0. \quad (6)$$

Here $\Pi_\mu = p_\mu - g_v \omega_\mu$ is the kinetic momentum, $m^* = M - g_s \Phi$ is the effective mass, and $F^{\mu\nu} = \partial^\mu \omega^\nu - \partial^\nu \omega^\mu$ is the field strength tensor. The distribution function is related to the scalar part of the Wigner function via

$$f(x, \Pi) = 4 \frac{\mathcal{F}(x, \Pi)}{m^*(x)}. \quad (7)$$

The vector part of the Wigner matrix can be obtained via

$$\mathcal{V}_\mu(x, \Pi) = \Pi_\mu \frac{\mathcal{F}(x, \Pi)}{m^*(x)}, \quad (8)$$

whereas the tensor part vanishes

$$\mathcal{S}_{\mu\nu}(x, \Pi) = 0. \quad (9)$$

The covariant Vlasov equation (5) can be solved as usual in transport theories by the test-particle method.¹⁷ From (5) it follows that if the distribution function $f(x, \Pi)$ is given by a sum over δ functions, i.e., a test-particle distribution, its time evolution is given by the test particles moving according to the following equations of motions:

$$\frac{\partial x^\mu}{\partial \tau} = \frac{\Pi^\mu}{m^*}, \quad (10)$$

$$\frac{\partial \Pi^\mu}{\partial \tau} = g_v \Pi_\nu \frac{F^{\mu\nu}}{m^*} + \partial_x^\mu m^*.$$

The equations of motion for the meson fields following from (1) are treated in the local density approximation. They are determined by

$$m_s^2 \Phi(x) + B \Phi(x)^2 + C \Phi(x)^3 = g_s \rho_s(x), \quad (11)$$

$$\omega_\mu(x) = \frac{g_v}{m_v} j_\mu(x),$$

with the nucleon current

$$\begin{aligned} j_\mu(x) &= 4 \int d^4 \Pi \mathcal{V}_\mu(x, \Pi) \\ &= \int d^3 \Pi \frac{\Pi_\mu}{\Pi_0} f(x, \Pi), \end{aligned} \quad (12)$$

where $j_0(x)$ is normalized to the total nucleon number, and the scalar density

$$\begin{aligned} \rho_s(x) &= 4 \int d^4 \Pi \mathcal{F}(x, \Pi) \\ &= \int d^3 \Pi \frac{m^*}{\Pi_0} f(x, \Pi). \end{aligned} \quad (13)$$

B. The two-body collision term

In principle, the collision term should be derived on equal footing with the streaming term by including two-particle correlations. Since such a stringent derivation is still a matter of debate¹⁸ we follow the covariant derivation in classical kinetic theory.¹¹ There the streaming term results from the consideration of particles moving on classical trajectories and the fact that the net flow through the surface of a Minkowski-space element given by the world lines of the particle vanishes. Therefore the Vlasov equation (5) propagates particles with mass m^* on trajectories (x_μ, Π_μ) . In the collision term one takes into account that these trajectories can change due to residual two-particle collisions which might account for the very short-range part of the nucleon-nucleon interaction.

The particular form of the collision term is based on the following assumptions.

(a) The hypothesis of molecular chaos ("Stosszahlansatz"), which assumes that the number of two-particle collisions is proportional to the one-body distribution functions of the colliding particles.

(b) The difference in the space-time coordinates of the particles before and after the collision can be neglected. This is in agreement with the assumption of smoothly

varying distribution function and meson fields which is necessary for the validity of the classical limit.

(c) The quantum mechanical Pauli principle is introduced via the blocking factors

$$\left[1 - \frac{(2\pi)^3}{4} f \right].$$

We thus obtain the following relativistic BUU equation:

$$\begin{aligned} & \{ \Pi_\mu \partial^\mu + [g_\nu \Pi_\nu F^{\mu\nu} + m^* (\partial_x^\mu m^*)] \partial_\mu^\Pi \} f(x, \Pi) \\ & = C(x, \Pi) \\ & = \int d^3 \Pi_1 d\Omega' \Pi_1^0 v \frac{d\sigma}{d\Omega} \left\{ f(x, \Pi') f(x, \Pi_1') \left[1 - \frac{(2\pi)^3}{4} f(x, \Pi) \right] \left[1 - \frac{(2\pi)^3}{4} f(x, \Pi_1) \right] \right. \\ & \quad \left. - f(x, \Pi) f(x, \Pi_1) \left[1 - \frac{(2\pi)^3}{4} f(x, \Pi') \right] \left[1 - \frac{(2\pi)^3}{4} f(x, \Pi_1') \right] \right\}, \end{aligned} \quad (14)$$

where the Møller velocity in the c.m. system of the colliding particles has the following form

$$v = |\mathbf{u} - \mathbf{u}_1| = \left| \frac{\mathbf{\Pi}}{\Pi_0} - \frac{\mathbf{\Pi}_1}{\Pi_1^0} \right| \quad (15)$$

and $|\mathbf{\Pi}'|$ and Π_1' depend on Π_1 and (Π^0, θ', ϕ') due to the four-momentum conserving δ function initially present in the expression for $C(x, \Pi)$. The evaluation of this δ function was performed for colliding particles with equal masses which is consistent with the second assumption above.

The factor $(2\pi)^3$ in the blocking factors is due to the normalization of the Wigner function [cf. Eq. (12)]. The factor $\frac{1}{4}$ comes from the spin and isospin degrees of freedom, which are not explicitly distinguished in the distribution function f .

One should note that the collision term depends on the kinetic momentum Π and not on the canonical momentum p . This is due to the fact that in the classical limit the kinetic momentum Π_μ is on the "effective mass shell" and is propagated via a classical equation of motion (10).

In a consistent theory the nucleon-nucleon cross section should be due to the exchange of the mesons appearing in the theory. In principle, it should therefore be calculated on the same basis as the mean field, also including medium effects. Since this is beyond the aim of the present contribution and also a very controversial subject⁴ we use the elastic free N - N cross section as a first approximation in the following, where we adopt the parametrization of Cugnon.¹⁹ One should note that in the present approach only the elastic part of the N - N cross section can be consistently taken into account. The inclusion of inelastic collisions, e.g., Δ excitations, would require an explicit treatment of the Δ degrees of freedom in the mean-field part.

III. NUMERICAL REALIZATION STABILITY TESTS

The numerical simulation of Eq. (5) together with (14) is based on the code of Bauer.²⁰ The initial configuration in coordinate space for a single nucleus is obtained by randomly distributing the test particles within a sphere of radius R . This radius is determined such that the single nucleus remains stationary during the time evolution. The smoothness of the surface is provided since the test particles also contribute with a certain fraction to the density at the nearest-neighbor grid points.²⁰ For the initialization in momentum space we use a local Fermi-gas model, where the density is assumed to have a Woods-Saxon shape. Tests with different initial configurations show that some observables might be somewhat sensitive to the initialization. The most accurate way would be to generate it from the Wigner transform of a self-consistent solution. However, for the following investigations, the present initialization scheme is found to be sufficient.

The time integration for the test-particle trajectories is performed by a predictor-corrector scheme with an error of $O(\Delta t^2)$, where one corrector step is found to be sufficient. Due to the momentum dependence of the mean field the predictor-corrector method is necessary to obtain the accuracy mentioned in contrast to the nonrelativistic case with a pure local mean field. For the bombarding energies considered in the following we use a time step size of $\Delta t = 0.2$ fm/c.

The evaluation of the fields and the densities is performed on a three-dimensional grid in coordinate space with $41 \times 41 \times 49$ grid points and a spacing of 1 fm. For this configuration we use 200 test particles per nucleon. The update of the scalar density after a time propagation of the test particles via (13) in general leads to a self-consistency problem since the effective mass depends again on the scalar density. We therefore iterate Eq. (13)

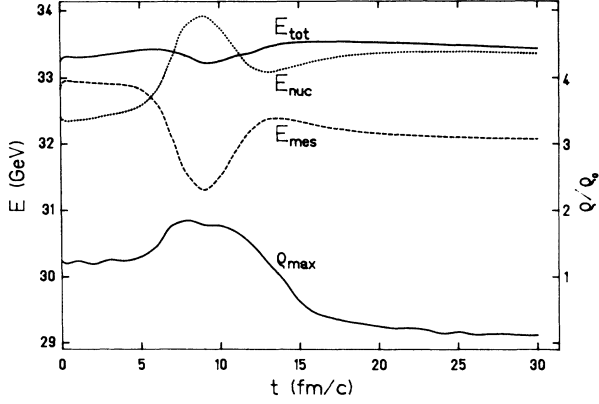


FIG. 1. Time evolution of the total energy E_{tot} , the nucleonic energy (including the interactions with the meson fields) E_{nuc} , and the meson field energy E_{meson} for a collision $^{16}\text{O} + ^{16}\text{O}$ at 600 MeV/nucleon ($b=0$). For the matter of representation we have shifted the zero energy level for E_{meson} by 32 GeV. The figure further contains the maximum density ρ/ρ_0 reached during the collision.

once in each update which is sufficient since for $\Delta t=0.2$ fm/c the density does not rapidly change between two time steps.

With this setup we find that a static nucleus remains numerically stable for a period of at least 30 fm/c which is relevant for the collisions considered in the following. Its total energy changes by 1% and the rms radius by 3%. This change is somewhat more pronounced than in a nonrelativistic calculation. This is due to the fact that in a relativistic model the nuclear potential, especially in the static case, is obtained as the sum of the two large contributions from the scalar and the vector field which nearly cancel.

In Fig. 1 we present the energies together with the maximum density for a head-on collision of $^{16}\text{O} + ^{16}\text{O}$ at 600 MeV including two-body collisions. We see that during the maximum overlap of the nuclei the meson energy decreases, which is due to the vanishing z component of the ω field in the overlap zone. This is balanced by the increase of the nucleon- ω interaction energy contained in E_{nuc} . The observed fluctuation in the total energy is also present in the pure Vlasov case. As already mentioned, it is due to the limited numerical accuracy in the treatment of the meson fields. However, since this fluctuation is maximally 1% of the total energy and small compared to the changes in the different energy contributions, the energy conservation is sufficient for the processes of interest.

IV. RESULTS

A. The time evolution in the Vlasov limit

We first focus on the results for the pure Vlasov part, i.e., the mean-field limit. Here we have used the following set of parameters from Refs. 9 and 13:

$$\text{(QHD I): } g_s = 9.57, \quad m_s = 2.79 \text{ fm}^{-1},$$

$$g_v = 11.67, \quad m_v = 3.97 \text{ fm}^{-1},$$

$$B = 0.0, \quad C = 0.0,$$

$$\text{(NLQHD): } g_s = 6.91, \quad m_s = 2.79 \text{ fm}^{-1},$$

$$g_v = 7.54, \quad m_v = 3.97 \text{ fm}^{-1},$$

$$B = -40.6 \text{ fm}^{-2}, \quad C = 384.4,$$

where QHD I leads to nuclear matter saturation at $\rho_0=0.19 \text{ fm}^{-3}$, an effective mass $m^*=0.56M$ and a compressibility of $K=540 \text{ MeV}$, and (NLQHD) to $\rho_0=0.145 \text{ fm}^{-3}$, $m^*=0.83M$ and $K=380 \text{ MeV}$. The corresponding EOS are given in Fig. 2.

In Fig. 3(a) we show the nucleon density during a head-on collision of two ^{16}O nuclei at 600 MeV/nucleon in the lab system. Here it is interesting to compare with the quantum mechanical mean-field calculation by Cusson *et al.*²¹ As in their work we observe an expanding system with decreasing density in the final state. However, the expansion is less isotropic and a target-like and projectile-like region can still be identified. This is also consistent with the momentum space distributions shown in Fig. 4, where the two Fermi spheres remain almost unchanged during the collision. The difference compared to Ref. 21 may thus be due to the classical limit or the local density approximation considered, especially since the latter neglects possible retardation effects.

We have further evaluated the transverse momentum in the reaction plane versus the longitudinal momentum to investigate the collective flow. In Fig. 5(a) we see that for the parameter set (QHD I) we obtain a high maximum value of about 1.2 fm^{-1} for the transverse momentum which is in agreement with Ref. 21. For the parameter set (NLQHD) one obtains a significantly reduced transverse momentum as also shown in Fig. 5(b). For the latter case, the maximum $p_t \approx 0.4 \text{ fm}^{-1}$ and is thus comparable to results with a Vlasov equation based on a non-relativistic Skyrme interaction (cf. e.g., Ref. 3). Thus, the high p_t obtained for QHD I is not due to the relativistic description of the collision as already pointed out in Ref.

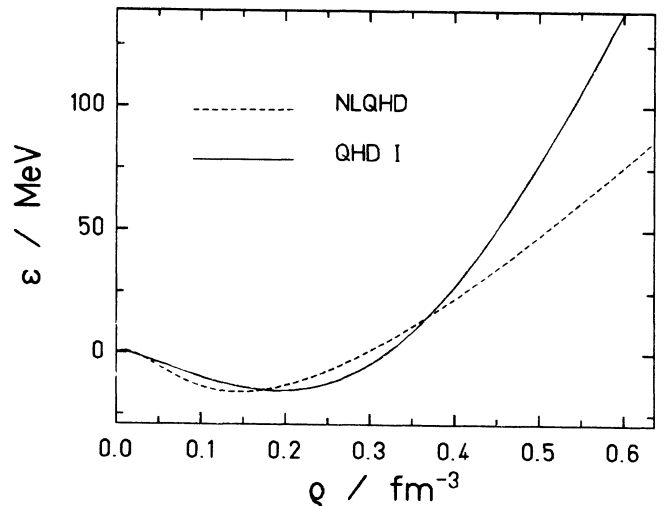


FIG. 2. The equations of state corresponding to the parameter sets (QHD I) and (NLQHD) taken from Refs. 9 and 13.

8, but rather has its origin in the dynamical properties of the Lagrangian density. This can be understood by the investigation of the maximum densities during the collision shown in Fig. 6. Although the two EOS do not differ significantly up to $2\rho_0$ we see that for NLQHD a higher maximum density is reached. This clearly shows

that the collision dynamics cannot be understood by the static properties of the EOS alone. The difference in the maximum densities must therefore be due to the more repulsive momentum dependence of QHD I ($m^*=0.56M$) compared to NLQHD ($m^*=0.83M$). This difference in the momentum dependence especially

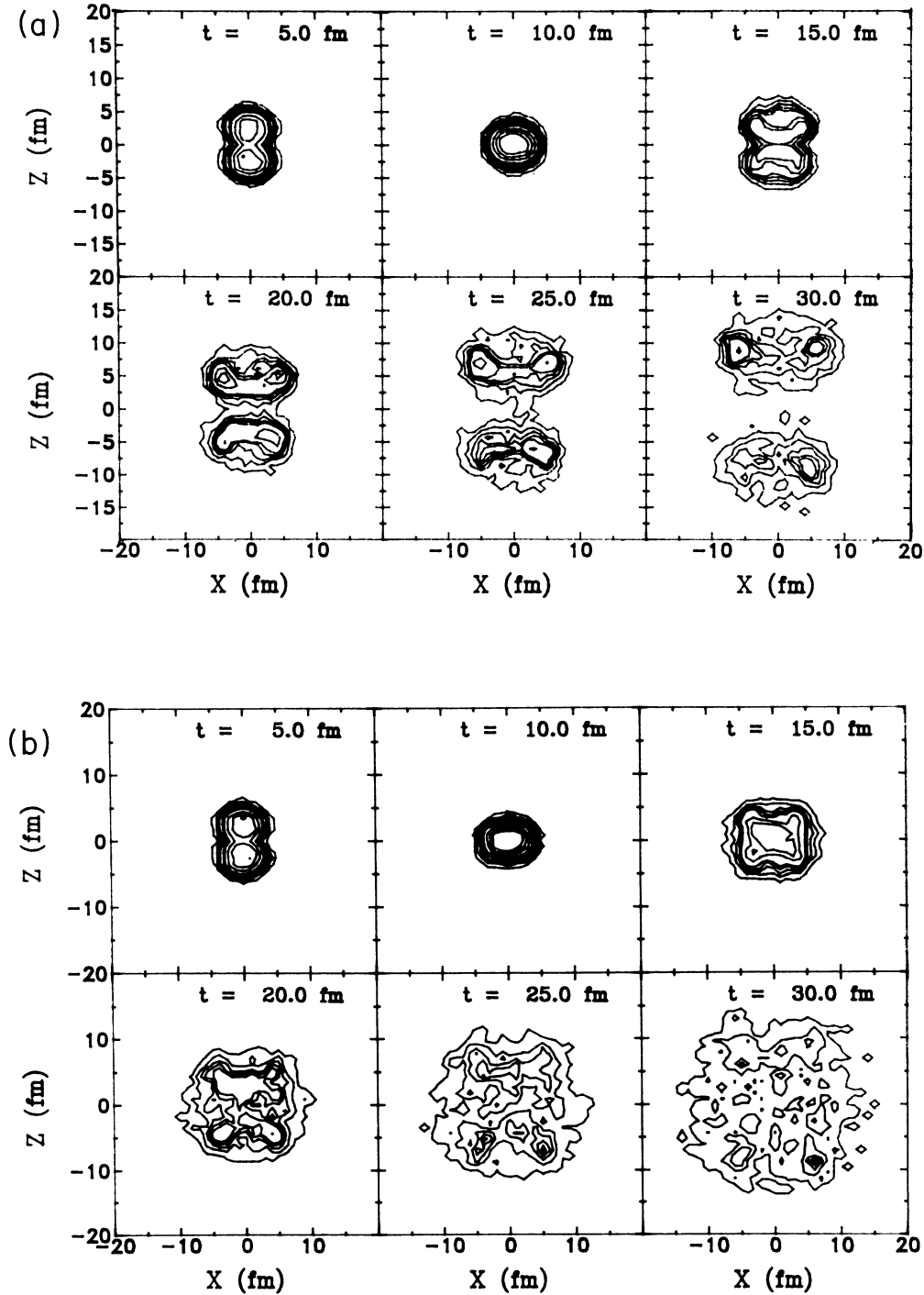


FIG. 3. Time evolution of the nucleon density for $^{16}\text{O}+^{16}\text{O}$ at 600 MeV/nucleon, (a) Vlasov limit, (b) including the collision term. The contour lines correspond to the following densities: 0.001, 0.005, 0.01, 0.015, 0.02, 0.04, 0.06, 0.12, 0.18, and 0.24 fm^{-3} .

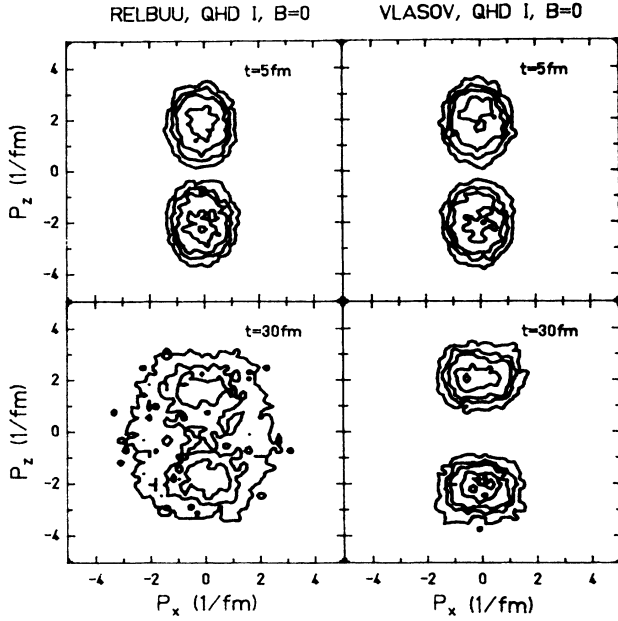


FIG. 4. Momentum space density $\int dp_x \rho(p_x, p_y, p_z)$ for the initial and final state of $^{16}\text{O} + ^{16}\text{O}$ at 600 MeV/nucleon in the collisionless case (VLASOV) and including two-body collisions (RELBUU). The contour lines correspond to densities 0.01, 0.05, 0.1, 0.2, 0.3, and 0.4 fm².

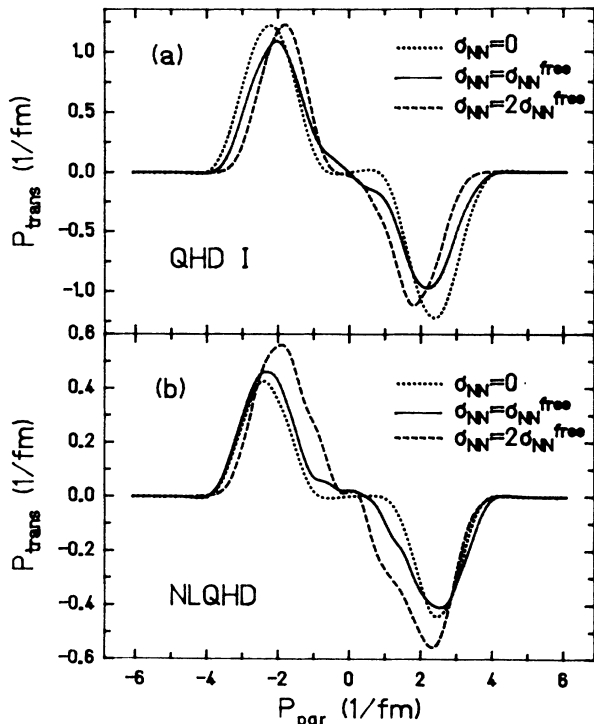


FIG. 5. Transverse momentum in the reaction plane vs longitudinal momentum for $^{16}\text{O} + ^{16}\text{O}$ at 600 MeV/nucleon and impact parameter $b=2$ fm; (a) QHD I, (b) NLQHD. Dotted curve; $\sigma_{NN}=0$ (Vlasov); solid curve, $\sigma_{NN}=\sigma_{NN}^{\text{free}}$; dashed curve, $\sigma_{NN}=2\sigma_{NN}^{\text{free}}$.

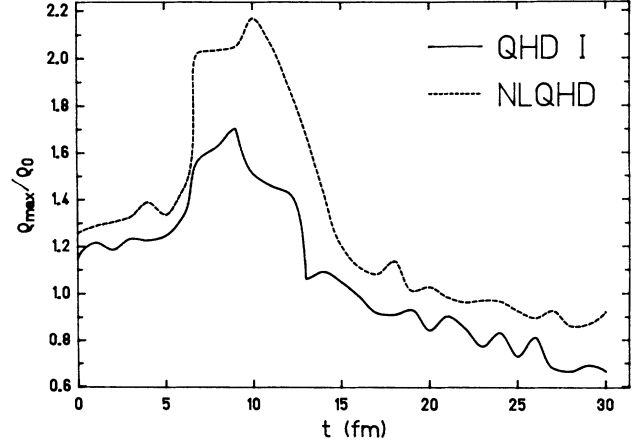


FIG. 6. Maximum density vs time for a collision $^{16}\text{O} + ^{16}\text{O}$ at 600 MeV/nucleon and $b=2$ fm calculated in the Vlasov limit: solid curve, QHD I; dashed curve; NLQHD.

explains the very large maximum p_t for QHD I. It strongly dominates over the higher static repulsion which should be felt by NLQHD because of the higher density reached. We note, however, that due to the linear energy dependence of the nucleon-nucleus optical potential this momentum dependence is overestimated for QHD I because of its low effective mass at bombarding energies above 250 MeV/nucleon.²²

Figure 5 further shows in the Vlasov limit for both parameter sets a flat momentum distribution around $p_{\text{par}}=0$. This is different from the result in Ref. 21 and indicates that the final configuration obtained within a pure Vlasov description does not contain any particles that are completely stopped which is also observed in the final momentum distribution in Fig. 4.

B. Results with the collision term

The effect of the collision term on the time evolution of the nucleon density for $^{16}\text{O} + ^{16}\text{O}$ at 600 MeV/nucleon is shown in Fig. 3(b). It turns out that, in contrast to the Vlasov case, the expansion after the collision is more isotropic and the density has strongly decreased. Thus the inclusion of two-particle collisions leads to a more thermalized final state and significantly reduces the transparency observed in the pure mean-field description. This is also obvious in the final momentum distribution (Fig. 4), where we observe a filling of the midrapidity region which indicates that particles have been stopped in the center-of-mass system. In the transverse momentum distribution (Fig. 5) this leads to the disappearance of the flat distribution around $p_{\text{par}}=0$.

The maximum transverse momentum is slightly reduced (QHD I) or remains constant (NLQHD) when the collision term is included (Fig. 5). This might be due to the increased stopping generated by the two-body collisions which leads to a reduced relative momentum of projectile and target when they overlap. Because of the momentum dependence of the mean field this then results in a less repulsive potential energy compared to the pure Vlasov limit. It is thus understandable that the effect is

more pronounced for (QHD I) than for (NLQHD).

To investigate the effects of possible medium corrections for the nucleon-nucleon cross section,⁴ we have repeated the calculations with twice the value of the free N - N cross section for σ_{NN} . In Fig. 5 we see that this results in a slight increase of the maximum p_t of about 5% for QHD I and a larger enhancement ($\approx 20\%$) for NLQHD. This raise in the transverse momentum is much smaller than observed by Bertsch *et al.*⁵ In their calculation for $^{40}\text{Ca} + ^{40}\text{Ca}$ at 400 MeV and $b=3$ for the mean transverse momentum was doubled when the assumed N - N cross section was multiplied by a factor of 2. However, this result was obtained for a momentum independent mean field. Thus, this observed enhancement of p_t is, in our case, compensated by the increased stopping which results in a less repulsive mean field. Due to this mechanism it turns out that for the two EOS considered and for $0 < \sigma_{NN} < 2\sigma_{NN}^{\text{free}}$ the transverse momentum distribution is much more affected by the properties of the mean field, especially its momentum dependence, than by the nucleon-nucleon cross section. Although the inclusion of the N - N collisions can significantly alter the reaction process as seen from the densities (Figs. 3 and 4) this is hardly seen in the maximum of the transverse momentum distribution.

In Fig. 7(a) we show the final rapidity spectrum in beam direction for the two different interactions. For the two cases no significant difference is observed. On the

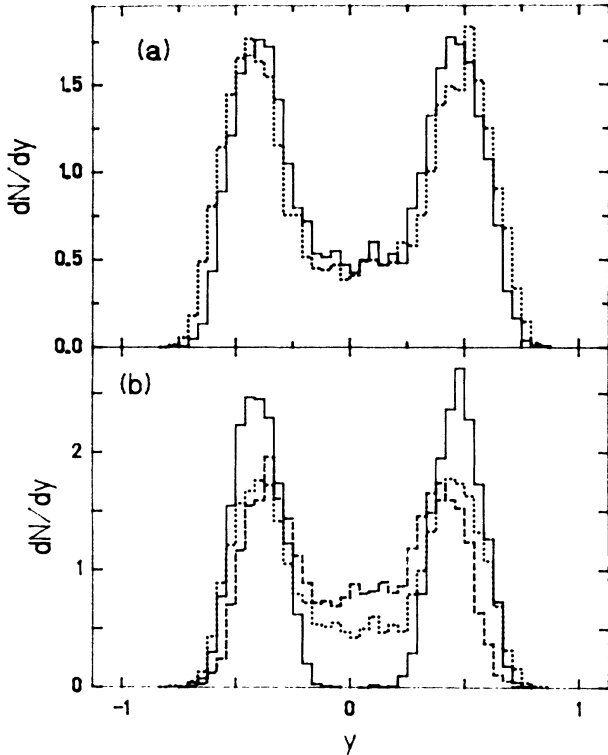


FIG. 7. Final rapidity spectrum for $^{16}\text{O} + ^{16}\text{O}$ at 600 MeV/nucleon for impact parameter $b=2$ fm; (a) $\sigma_{NN} = \sigma_{NN}^{\text{free}}$; solid line, QHD I; dotted line, NLQHD. (b) QHD I; solid curve, $\sigma_{NN} = 0$ (Vlasov); dotted curve, $\sigma_{NN} = \sigma_{NN}^{\text{free}}$; dashed curve, $\sigma_{NN} = 2\sigma_{NN}^{\text{free}}$.

other hand, the rapidity distribution is much more sensitive to two-body collisions as demonstrated in Fig. 7(b), where we show results for $\sigma_{NN} = 0$ (Vlasov), $\sigma_{NN} = \sigma_{NN}^{\text{free}}$, and $\sigma_{NN} = 2\sigma_{NN}^{\text{free}}$. We find that an increase of the cross section leads to a stronger equilibration, i.e., a filling of the midrapidity region. A qualitatively similar result has been formed by Rosenauer *et al.*²³ within the nonrelativistic quantum molecular dynamics model.

C. Application to hard photon production

We have further applied our model to the production of high energy photons in heavy-ion collisions. Following the work of Bauer *et al.*²⁴ we assume that the photons are produced by incoherent p - n bremsstrahlung. For the elementary $pn \rightarrow pn\gamma$ cross section we adopt the hard-sphere collision limit as in Ref. 24. Inclusive double differential photon yields then are evaluated by summing over each individual p - n collision as described in Ref. 24 and integrating over the impact parameter. In Fig. 8 we show the results for $^{16}\text{O} + ^{16}\text{O}$ at a bombarding energy of 250 MeV/nucleon, remaining below the energy range where the Δ excitation has to be taken into account. For low γ energies the cross section obtained with QHD I is somewhat larger than for NLQHD, whereas at higher γ energies the difference totally disappears. However, even at small energies this difference is not very significant and is due to the cancellation of different effects. On one hand, the increased stopping for QHD I leads to smaller relative nucleon momenta available for the photon production. On the other hand, the semiclassical $pn \rightarrow pn\gamma$ cross section is proportional to the square of the proton velocity. Since, for a given momentum, the particle with the lower effective mass has the higher velocity, this increases the photon yield for QHD I such that the decrease due to the stopping is compensated and a small net enhancement remains. We therefore obtain a different result than in a previous work¹² where this effect was not taken into account.

The different effective masses further result in different momentum distributions for the boosted systems. Since the momentum in beam direction Π'_z of a boosted nucleon is obtained from Π_z and Π_0 in the rest frame of the nucleus via

$$\Pi'_z = \gamma(\beta\Pi_0 + \Pi_z) \quad (16)$$

the higher effective mass for NLQHD leads to a higher Π_0 and thus to higher momentum tails. For high photon energies this then compensates for the larger elementary production cross section for QHD I and leads to the same γ yield for both EOS.

V. SUMMARY AND CONCLUSION

We have presented a covariant transport theory based on the σ - ω model and a collision term introduced along the line of relativistic classical kinetic theory. The model is thus appropriate for the investigation of heavy-ion collisions at high energies (SIS and BEVALAC regime) and allows for a consistent inclusion of a momentum dependence of the interaction. We have obtained an insight

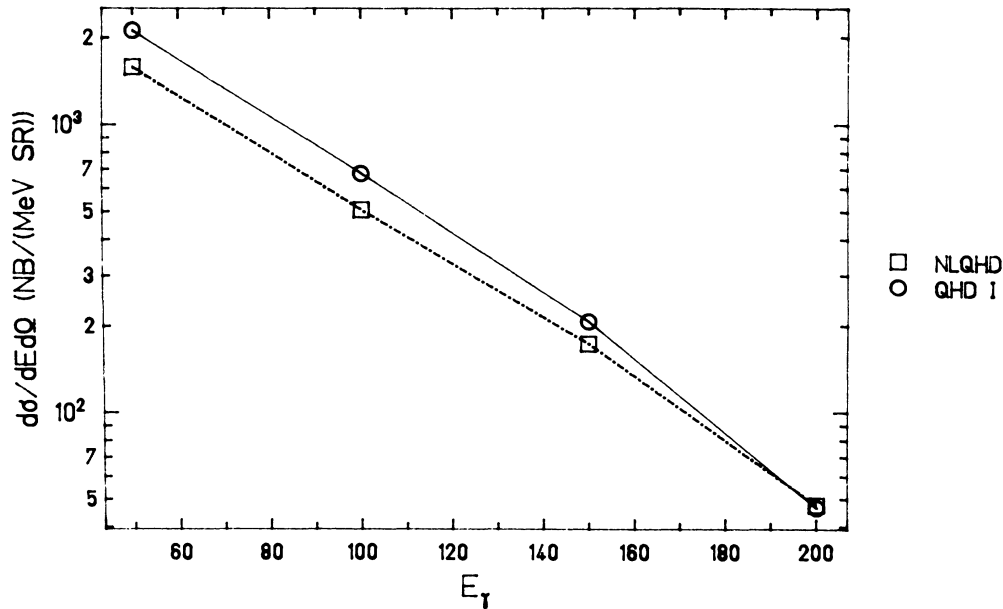


FIG. 8. Photon cross section vs photon energy at $\theta_{\text{lab}}=90^\circ$ for $^{16}\text{O}+^{16}\text{O}$ at 250 MeV/nucleon; circles, QHD I; squares, NLQHD.

into the effects arising from a relativistic mean-field description and the inclusion of two-body collisions. In this context the most striking result is the importance of the momentum dependence of the interaction for the transverse momentum distribution. We find that the high p_t obtained with the parameter set QHD I can be significantly reduced with the parameter set NLQHD involving a higher effective mass which leads to a less repulsive momentum dependence. Therefore, the higher transverse momentum for QHD I is not mainly due to the relativistic description but rather stems from the repulsive momentum dependence of the mean field which is in agreement with the results obtained by Ko *et al.*¹³ The influence of the collision term on the p_t spectrum is less pronounced, at least for the relative light nuclei considered. Even an increase of the N - N cross section by a factor of 2 only leads to a slight increase of the maximum p_t . This result is due to an interplay between the increased stopping, which leads to a reduction of the transverse momentum, and a direct increase of p_t due to two-particle collisions as observed in a calculation with a momentum independent mean field.⁵

The high-energy photon spectra calculated with the two parameter sets showed a difference for the lower γ energies which has its origin in the sensitivity of the elementary production cross section to the effective mass. This leads to the, at first sight, astonishing result that more photons are produced for the more repulsive EOS (QHD I). However, one should note that this difference is not very pronounced and a quantitative comparison with experiment requires further investigations, e.g., on the elementary production cross section.

In summary, our results show that the observables from high-energy heavy-ion collisions are sensitive to

various parameters which enter into the description. Thus a serious determination of the EOS requires much further effort. Especially the interplay between the nucleon-nucleon collisions, e.g., the N - N cross section and the momentum dependence of the mean field, is essential for extracting information about the EOS from measured transverse momentum distributions. Here the presented approach can serve as a good starting point in this direction, since it is formulated covariantly and contains the momentum dependence in a consistent way. In principle, it can further be extended to include a more consistent and theoretically founded collision term. However, this will require more insight into the medium corrections of the nucleon-nucleon cross section. Also the momentum dependence of the optical potential at higher densities has to be investigated carefully and adjusted to the experimental data.²² The underlying field theoretical model should also be extended to include the delta resonance and further mesons, especially the pion. Finally one has to investigate the effects of the full solution of the corresponding meson field equations, i.e., relativistic retardation effects, as well as distortions in the negative energy sea during the collision process.

ACKNOWLEDGMENTS

We would like to thank W. Bauer for introducing us to his BUU code, and his help in the early stage, K. Niita for further advice, as well as Professor X.-Z. Zhang for useful discussions. One of us (V.K.) would further like to thank the Nuclear Theory Group in Stony Brook for the warm hospitality. During this time he was supported by the German academic exchange service (DAAD). This work was supported by BMFT and GSI Darmstadt.

- ¹F. G. Perey, Phys. Rev. **131**, 745 (1963); G. E. Brown, J. S. Dehesa, and J. Speth, Nucl. Phys. **A330**, 290 (1979); C. Mahaux and H. Ngo, Phys. Lett. **100B**, 285 (1981); M. Bauer, E. Hernandez-Saldana, P. E. Hodgson, and J. Quintanilla, J. Phys. G **8**, 525 (1982).
- ²K. A. Brueckner, Phys. Rev. **97**, 1353 (1955); H. A. Bethe, *ibid.* **103**, 1353 (1956); H. A. Bethe and J. Goldstone, Proc. Roy. Soc. London, Ser. A **238**, 551 (1957).
- ³C. Gale, G. Bertsche, and S. Das Gupta, Phys. Rev. C **35**, 1666 (1987); J. Aichelin, A. Rosenhauer, G. Peilert, H. Stöcker, and W. Greiner, Phys. Rev. Lett. **58**, 1926 (1987).
- ⁴G. E. Brown and V. Koch, Proceedings of the 8th High Energy Heavy Ion Study, Lawrence Berkeley Laboratory, Report LBL-24580, edited by J. W. Harris and G. J. Wozniak, p. 29.
- ⁵G. F. Bertsch, W. G. Lynch, and M. B. Tsang, Phys. Lett. B **189**, 384 (1987); B. Schürmann, Technische Universität München, Report 22, 1988.
- ⁶E. Osnes and D. Strottman, Phys. Lett. **166B**, 5 (1986).
- ⁷T. A. Ainsworth, E. Baron, G. E. Brown, J. Cooperstein, and M. Prakash, Nucl. Phys. **A464**, 740 (1987).
- ⁸V. Koch, U. Mosel, T. Reitz, Chr. Jung, and K. Niita, Phys. Lett. **206B**, 395 (1988).
- ⁹B. S. Serot and J. D. Walecka, Adv. Nucl. Phys. **16**, 1 (1986).
- ¹⁰H.-Th. Elze, M. Gyulassy, D. Vasak, H. Heinz, H. Stöcker, and W. Greiner, Mod. Phys. Lett. **2**, 451 (1987).
- ¹¹S. R. de Groot, W. A. Leewen, and Ch. G. van Weert, *Relativistic Kinetic Theory* (North-Holland, Amsterdam, 1980).
- ¹²B. Blättel, V. Koch, W. Cassing, and U. Mosel, Proceedings of the International Workshop on Gross Properties of Nuclei and Nuclear Excitations XVI, Hirschegg, Austria, 1988, edited by H. Feldmeier, p. 79.
- ¹³C. M. Ko, Q. Li, and R. Wang, Phys. Rev. Lett. **59**, 1084 (1987); C. M. Ko and Q. Li, Phys. Rev. C **37**, 2270 (1988).
- ¹⁴J. Boguta and A. R. Bodmer, Nucl. Phys. **A292**, 413 (1977); J. Boguta and H. Stöcker, Phys. Lett. **120B**, 289 (1983); B. M. Waldhauser, J. A. Maruhn, H. Stöcker, and W. Greiner, University of Frankfurt Report UFTP 195, 1987.
- ¹⁵T. Matsui, Nucl. Phys. **A370**, 365 (1981).
- ¹⁶D. Vasak, M. Gyulassy, and H.-Th. Elze, Ann. Phys. (N.Y.) **173**, 462 (1987).
- ¹⁷C. Y. Wong, Phys. Rev. C **25**, 1460 (1982); G. Bertsch, H. Kruse, and S. Das Gupta, *ibid.* **29**, 673 (1984).
- ¹⁸W. Botermans and R. Malfliet, Proceedings of the 8th Balaton Conference on Nuclear Physics, 1987, edited by Z. Fodor, p. 86.
- ¹⁹J. Cugnon, T. Mizutani, and J. Vandermeulen, Nucl. Phys. **A352**, 505 (1981).
- ²⁰W. Bauer, Ph.D. thesis, Justus-Liebig-Universität Giessen, 1987 (unpublished).
- ²¹R. Y. Cusson, P.-G. Reinhard, J. J. Molitoris, H. Stöcker, and W. Greiner, Phys. Rev. Lett. **55**, 2786 (1985); J. J. Bai, R. Y. Cusson, J. Wu, P.-G. Reinhard, H. Stöcker, and W. Greiner, Z. Phys. A **326**, 269 (1987).
- ²²C. J. Horowitz, Proceedings of the International Workshop on Gross Properties of Nuclei and Nuclear Excitations XVI, Hirschegg, Austria, 1988, edited by H. Feldmeier, p. 10.
- ²³A. Rosenhauer, G. Peilert, H. Stöcker, and W. Greiner, University of Frankfurt Report UFTP 203, 1987.
- ²⁴W. Bauer, G. F. Bertsch, W. Cassing, and U. Mosel, Phys. Rev. C **34**, 2127 (1986).